Construction and characteristics of stainless steel/calcium silicate manufactured by selective laser melting

Ma Zhengjie

School of Material Science and Engineering, Tongji University, Shanghai 200092, China
laonawugen@163.com

Abstract: The Selective Laser Melting is a branch of 3D printing. By maneuvering the layered data of the 3D model, the computer is capable of melting the sheer layer power with the high energy laser beam and then forming superposition layer by layer. Compared to traditional processing methodologies, the SLM technique stands out for its high-precision, high customization, and complex internal structure to become the perfect candidate for bone implantation. To explore and produce the perfect stainless steel compound ($nCaSiO_3$) for the SLM bone repairing implants, we are focusing on its physical and chemical performances, such as excellent biocompatibility, corrosion resistance capability, compact structure, and mechanical properties. We concluded the research directions as below: (1) We have successfully prepared the composite powder material - 316 L/$nCaSiO_3$ of different ratio and proportions using the high energy ball-milling technique. Plus, we have made the nanometer $CaSiO_3$ powder disperse and form a stable layer on the 316L stainless steel matrix powder. (2) Based on the fact that we can produce the 316L/ $nCaSiO_3$ composite powder, we probed into the influences of factors on the production of the composite microstructure. The factors include the process parameters of SLM and various levels of $CaSiO_3$ concentrations. Because of the temperature gradient of the composite powder in the furnace hearth, equiax crystal and dendrite would form inside the material during the process. In addition, along with the increasing content of $CaSiO_3$, the number of defects in the internal material increases and the density of defects goes up.

[Ma Zhengjie. **Construction and characteristics of stainless steel/calcium silicate manufactured by selective laser melting.** *J Am Sci* 2017;13(8):113-119]. ISSN 1545-1003 (print); ISSN 2375-7264 (online). http://www.jofamericanscience.org. 14. doi:10.7537/marsjas130817.14.

Keywords: 316L stainless steel, SML Selective Melting Laser, Composite Powder Material，Microstructure

1. Introduction

Beside other characterizations, properties, metal-bioceramic biomedical composites also have excellent mechanical properties and excellent properties of ceramics, which opens up a new way to prepare human implant materials. 316L austenitic stainless steel has a good comprehensive mechanical properties, easy processing, low price characteristics [1-2], at home and abroad as early as the human body hard tissue repair and implantation of a class of materials, and are more used in artificial implantation of bones, cardiovascular stent, orthopedic stent, implant and so on [3]. In clinical applications, there are still several problems: 1. Biocompatibility is poor; 2. Corrosion resistance to be improved; 3. There is stress shielding [4-6]. Bioceramics are currently clinically used to repair and reconstruct diseased or damaged skeletal systems, which have excellent corrosion resistance, biocompatibility and osteoinduction [7]. But at the same time biocoramic comprehensive mechanical properties are poor, as a single material prepared by the skeleton in the load-bearing and other significant defects [8]; In addition, the ceramic preparation process is complex and poor processability, which are limited as a bone repair material Application [9]. Therefore, the use of 316L stainless steel / bioceramics prepared composite materials, on the one hand with excellent physical and mechanical properties of metal materials, on the one hand due to the addition of bioceramics, make up for the metal materials, biocompatibility and poor corrosion resistance [10-11]. In this paper, the study object is a 316L stainless steel / bioceramic composites for human skeletal plants. The composite bulk materials are prepared by high energy ball milling and SLM technology. The composite materials are prepared by subjecting the powder and bulk material with different content and forming conditions. The microstructure and the microstructure and structure of the 316L stainless steel / calcium silicate composite medical biomaterial were designed and fabricated to optimize the design of the composite material.

2. Surface appearance and microstructure of materials

In order to further study the properties of the prepared powder material and the bulk material, the influence of the technological parameters and the content of calcium silicate on the material was determined. The surface and microstructure of the material were observed and analyzed by SEM, EDS and XRD.

The surface morphology of the composite powder after ball milling and vacuum drying was observed under scanning electron microscope, as shown in Figure 1. It can be seen from the figure, after

mechanical milling, the composite powder particles to maintain a good spherical shape, but 316L stainless steel powder surface becomes rough. $CaSiO_3$ powder is mostly coated on the surface of stainless steel particles, a small part of the scattered between the stainless steel particles or with stainless steel particles agglomerate into irregular shape. Compared with Figure 1 (a) and (b) and (c), it was found that with the increase of $CaSiO_3$ powder content, the agglomeration was more obvious and the sphericality of the particles decreased. The surface energy spectra of the surface of 316L / $5CaSiO_3$ particles were further characterized by the surface energy spectrum of $CaSiO_3$ powder on the surface of stainless steel particles, and the surface energy spectrum was obtained as shown in Figure 2 (c), (d) and (e) are the results of energy spectrum analysis of Ca, Si and Fe elements, respectively. (2) (b) is the high magnification of the red box region in (a). It can be seen from Figure 2 that Ca, Si elements are uniformly distributed on the surface of Fe and the roughness is low, and there is no obvious spheroidization phenomenon when the ratio of n = 5, that is, 316L stainless steel powder and nanometer calcium silicate powder is 95:5.

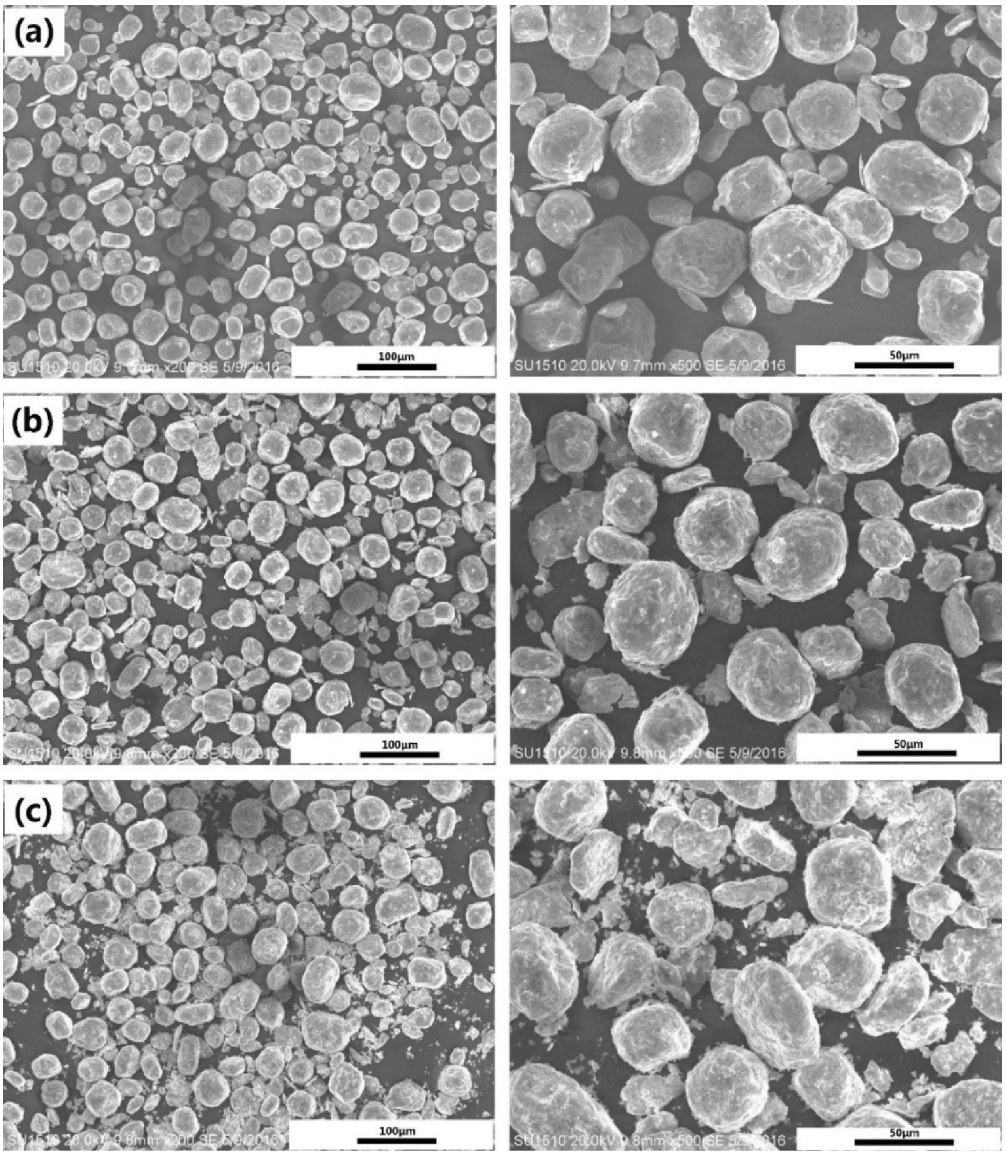

Figure 1. Surface morphology of 316L / nCaSiO3 ((a): n = 5, (b): n = 10, (c): n = 15)

The results of point spectrum analysis of small particles in the composite powder are shown in Figure The object was selected as 316L / $15CaSiO_3$ composite powder. It can be seen from the results of energy spectrum analysis that the main constituent elements of 316L / $15CaSiO_3$ powder are O, Si, Ca and a small amount of Fe and Cr elements, indicating that the small particles are mainly agglomerated with

$CaSiO_3$ powder coated on the surface of 316L stainless steel The formation of irregular shapes.

3. Analysis of Surface Morphology and Microstructure of Bulk Materials

3. 1 Analysis of Surface Morphology of Block Material

The overall morphology of the specimen was observed with a low magnification, and the results are shown in Figure. It can be seen that with the increase of the laser power, the size of the defect hole is rapidly reduced. Further observation with high magnification lens under different laser power pure 316L stainless steel block surface morphology defects shown in Figure 5. In the low laser power forming conditions, the sample surface rough and porous. 120W, due to the low power of the laser, the energy is low, the bath temperature is low, the powder is not completely melted and the spreadability is poor, there are a lot of unmelted powder in the molten pool, which can not be fused with the laser cladding layer. The progress of the forming process, the defect is connected to form the large hole defects in Figure 5 (a). In Figure 5 (b), when the laser power is increased to 140W, the diameter of the pores is remarkably reduced, and almost no unmelted powder is present, but there are still significant defects. When the power increases to 160W, the sample surface only sporadic hole defects exist, and the overall appearance of the smooth, adjacent cladding lines between the melting pool or overflow phenomenon, as shown in Figure 5 (c) below. And when the power is further increased to 180W, due to the laser energy is too high, the powder melting part of the powder is adsorbed to the surface of the cladding line, so that the gap between the welding line melting pool phenomenon, as shown in Figure 5 (d) In this case, the resulting molded article is unstable. Therefore, in the choice of forming laser power can not be too low, there will be a lot of defects, reduce the sample strength; can not be too high, so that the sample performance is not stable, the ideal laser power in this experiment is 160W.

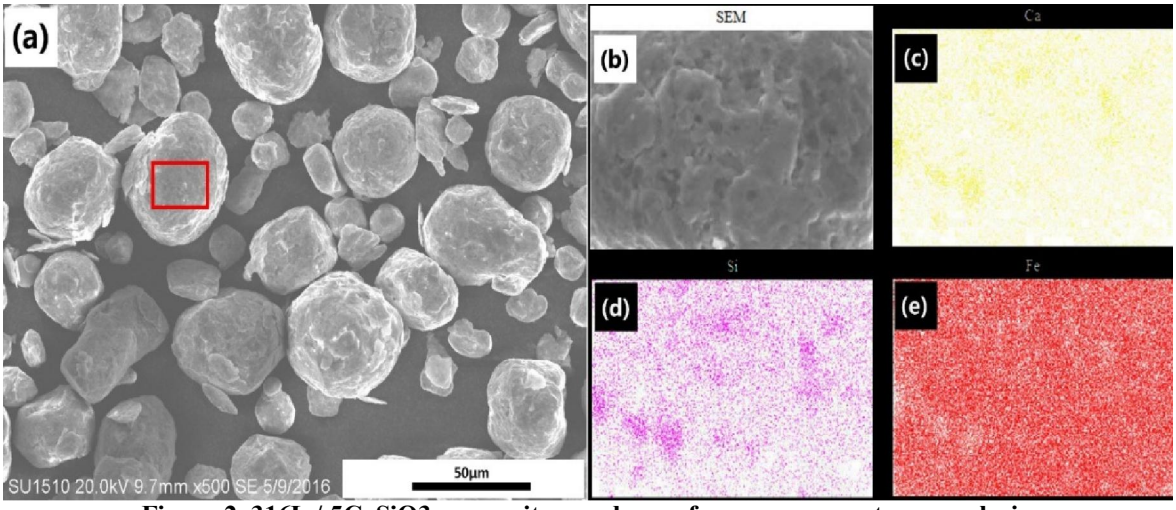

Figure 2. 316L / 5CaSiO3 composite powder surface energy spectrum analysis

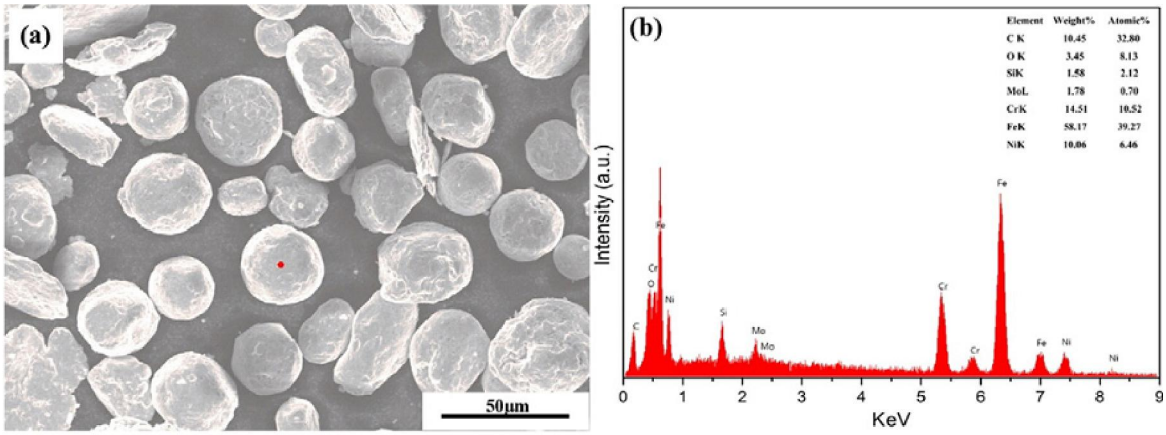

Figure 3. Point spectrum analysis of 316L / 15CaSiO3 composite powder

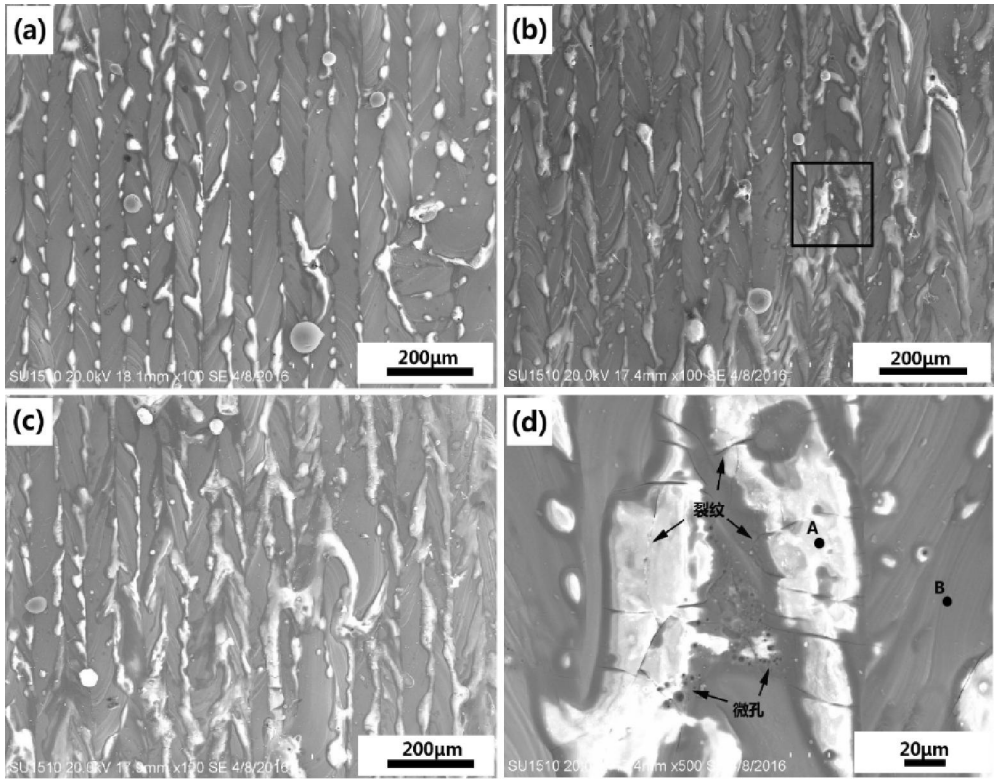

Figure 4. Original surface morphology of composite samples observed at low magnification microscopy with different weight percentage of $CaSiO_3$ （（a）0, (b) 5%, (c) 10%, (d) 15%）

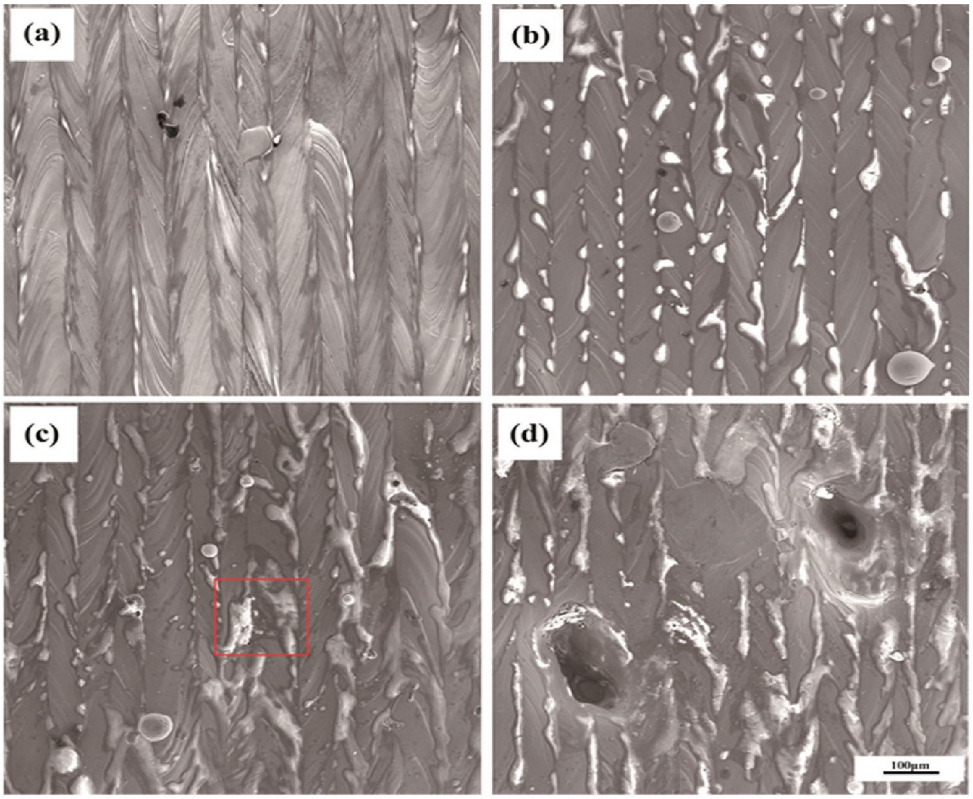

Figure 5. Original surface morphology of a 316L stainless steel sample observed with a high power microscope at different laser power （（a）120w, (b) 140w, (c) 160w, (d) 180w）

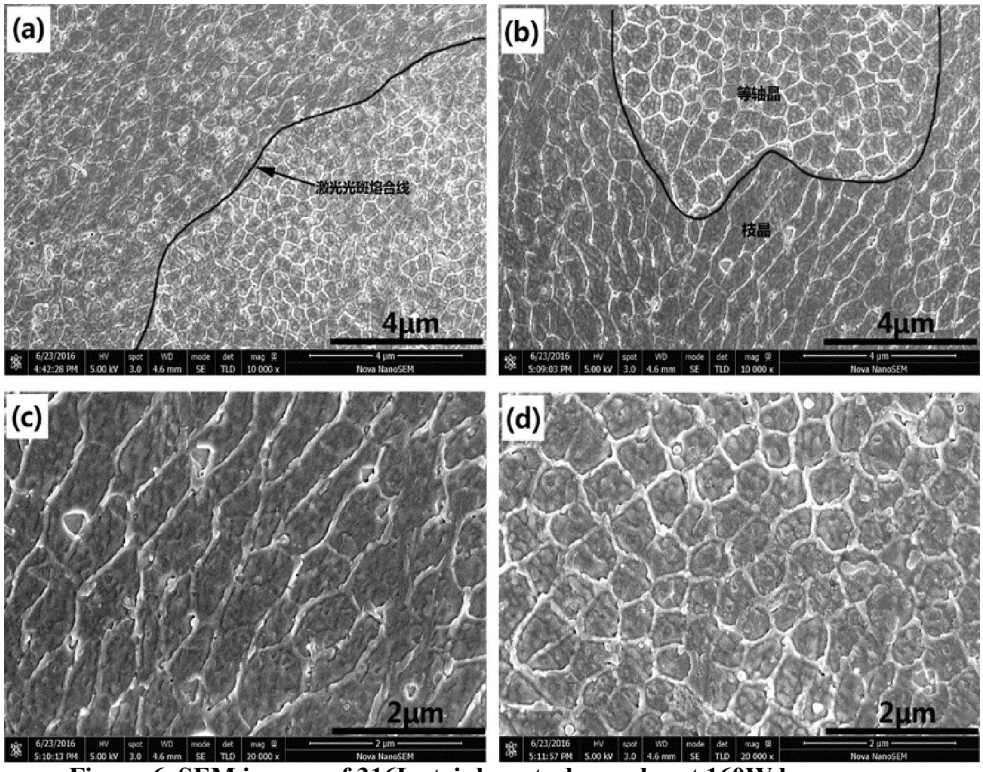

Figure 6. SEM images of 316L stainless steel samples at 160W laser power

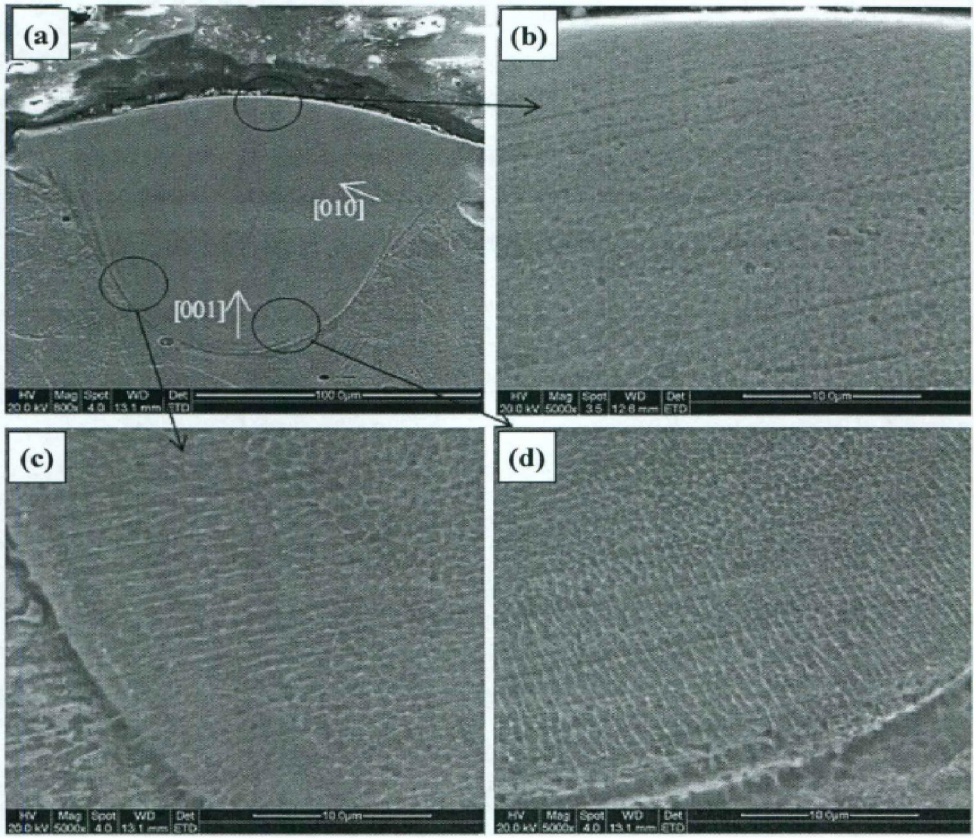

Figure 7. SEM photograph of 316L stainless steel single-channel cladding strip longitudinal section

The spheroidizing effect in the process of preparing the bulk material of the SLM will affect the performance and final formation of the sample. The spheroidizing effect is caused by the formation of the sample surface due to the surface tension or wettability of the molten metal during the preparation of the sample Metal ball phenomenon [12]. The spheroidization effect makes the surface of the sample rough, and its effect on the sample will continue to accumulate, and ultimately may lead to forming failure According to the related literature, the main reason for the formation of spheroidization is that the oxide film on the surface of the molten layer hinders the adhesion between layers, which can be effectively reduced by reducing the oxygen content in the raw material, increasing the laser power, reducing the laser scanning speed, and laser repeating scanning Spheroidization [13-14].

3.2 Analysis of Brick Material Structure

The microstructure of the 316L stainless steel block sample at 160W laser power was observed by SEM as shown in Figure 6, where Figure 6(a) is a SEM photograph of the molten pool area of 316L stainless steel block sample, (b) is the sample pool area SEM images of equiaxed and dendrites, (c) SEM images of molten pool area, and (d) is SEM images of molten pool area. Figure 6(a) and (b) show that there is a clear boundary between the equiaxed grains and the dendrites (black lines), and the dendrites and equiaxed grains are well bonded. Dendrites are radially divergent toward the pool boundary and are interrupted at the boundary, and the equiaxed grains grow to the dendrites of the boundary. In the high-power electron microscope, the equiaxed crystal and dendritic morphology at the boundary are shown in Figure 6(c) and (d). It can be seen that the transition of partial dendrites to equiaxed grains is due to the interfacial temperature gradient The dendrites that have grown horizontally have been solidified, and some of the dendritic growth direction is deflected and grown to the equiaxed portion.

The longitudinal section of 316L stainless steel single-channel cladding line was observed by SEM as shown in Figure 7. Figure 7 (a) is a single-channel cladding line, (b) (c) (d) are the photographs of the area shown in (a) above the high magnification electron microscope, respectively. It can be clearly seen that the formation of single-wall cladding lines at different locations to form a completely different morphology. The upper region of the molten pool shown in Figure 7 (b) is mainly equiaxed and has a dendritic structure in the molten pool boundary region shown in Figure 7 (c) (d), and the growth direction is perpendicular to the boundary. In the process of SLM forming, the molten pool is formed after the laser beam melts the powder material. The farther away from the laser center in the molten pool, the smaller the temperature field, the laser energy at the boundary of the molten pool can make the powder material reach the melting point. The heat is transferred through the heat transfer in the molten pool, and the heat is transmitted perpendicularly to the boundary during the heat transfer process, thus forming the dendritic grain growth mode at the boundary perpendicular to the boundary. Due to the strongest heat dissipation at the boundary, the maximum temperature gradient, and the solidified part of the non-solidified metal liquid to provide nucleation core, so the border to the growth rate of the fastest. In the pool, the heat dissipation is weakened and the temperature gradient is gentle. Therefore, when the atoms are enriched in the phase, the supercooling of the solid-liquid interface gradually increases to a sufficiently heterogeneous nucleation. Compared with dendritic crystal structure, equiaxed crystal grains are small, with good strength and toughness, excellent mechanical properties, and isotropic, the performance is more stable.

4. Summary

Based on the successful preparation of 316L / $nCaSiO_3$ composite powder and bulk materials, the effects of various process parameters and CaSiO3 content on the structure and appearance of the samples were studied. The experiment was applied to the industrial production applications Of the production parameters, get the main conclusions are as follows:

(1) The dispersion of nanometer $CaSiO_3$ powder in 316L stainless steel matrix powder was determined by studying the surface appearance and particle size distribution of the powdery material.

(2) Microstructure of bulk material was observed by SEM, and the microstructure of the bulk material was determined as a dendritic crystal and equiaxed crystal according to the electron microscope. The dendrites were grown at the boundary of the molten pool and perpendicular to the boundary of the molten pool. Located inside the pool;

(3) Considering the material density, surface appearance defects, microstructure and other factors to get the ideal process parameters for the 5% CaSiO3 content, laser power 160W, scanning speed 400mm / s, then get the material density is high, Less defects and no large-size holes, the internal can form a large number of equiaxed crystal.

References

1. Sun Jian-hua, Liu Jin-long, Wand Qing-liang, Wu Gao-feng. Study on Surface Modification of Medical 316L Stainless Steel [J]. Materials Review, 2011, (09): 95-98.

2. Cardenas L, MacLeod J, Lipton-Duffin J. Reduced graphene oxide growth on 316L stainless steel for medical applications [J]. Nanoscale, 2014, 6(15): 8664-8670.
3. Hao L, Dadbakhsh S, Seaman O. Selective laser melting of a stainless steel and hydroxyapatite composite for load-bearing implant development [J]. Journal of Materials Processing Technology, 2009, 209(17): 5793-5801.
4. Chen Demin. Bioceramic materials [J]. Journal of Oral Materials Instruments, 2005, (03): 157-158.
5. Chen H, Clarkson B, Sun K et al. Self-assembly of synthetic hydroxyapatite nanorods into an enamel prism-like structure [J]. Journal of Colloid and Interface Science, 2005, 288(1): 97-103.
6. Yu Jia, Yu Jianchang, Huang Qingming, Yi Xiaohong, Fu Yanqiu. Preparation and characterization of one-dimensional nano-hydroxyapatite [J]. China Ceramics, 2009, (10): 34-36.
7. Dong L, Wang H. Microstructure and corrosion properties of laser-melted deposited Ti2Ni3Si/NiTi intermetallic alloy [J]. Journal of Alloys and Compounds, 2008, 465(1-2): 83-89.
8. Li Ruidi, Shi Yusheng, Wang Zhigang, et al. Densification behavior of gas and water atomized 316L stainless steel powder during selective laser melting [J]. Applied Surface Science, 2010, 256: 4350-4356.
9. Yan Zhagong, Lin Feng, Qi Haibo, Yan Yongnian. Direct metal rapid prototyping manufacturing technology [J]. Journal of Mechanical Engineering, 2005, (11): 5-11.
10. Wang Li. Selective laser melting forming metal parts performance research [D]. Huazhong University of Science and Technology, 2012.
11. Kempen K, Thijs L, Van Humbeeck J et al. Processing AlSi10Mg by selective laser melting: parameter optimisation and material characterisation [J]. Materials Science and Technology, 2014, 31(8): 917-923.
12. Das S. Physical Aspects of Process Control in Selective Laser Sintering of Metals [J]. Advanced Engineering Materials, 2003, 5(10): 701-711.
13. Li R, Liu J, Shi Y et al. Balling behavior of stainless steel and nickel powder during selective laser melting process [J]. The International Journal of Advanced Manufacturing Technology, 2011, 59(9-12): 1025-1035.
14. Yap C, Chua C, Dong Z et al. Review of selective laser melting: Materials and applications [J]. Applied Physics Reviews, 2015, 2(4): 041101.

8/25/2017